Actinide Chemistry

Deutsche Ausgabe: DOI: 10.1002/ange.201607022
Internationale Ausgabe: DOI: 10.1002/anie.201607022

Subtle Interactions and Electron Transfer between U^{III}, Np^{III}, or Pu^{III} and Uranyl Mediated by the Oxo Group

Polly L. Arnold, Michał S. Dutkiewicz, Markus Zegke, Olaf Walter, Christos Apostolidis, Emmalina Hollis, Anne-Fréderique Pécharman, Nicola Magnani, Jean-Christophe Griveau, Eric Colineau, Roberto Caciuffo,* Xiaobin Zhang, Georg Schreckenbach,* and Jason B. Love**

Abstract: *A dramatic difference in the ability of the reducing An^{III} center in $AnCp_3$ (An = U, Np, Pu; Cp = C_5H_5) to oxo-bind and reduce the uranyl(VI) dication in the complex [(UO_2)(THF)(H_2L)] (L = "Pacman" Schiff-base polypyrrolic macrocycle), is found and explained. These are the first selective functionalizations of the uranyl oxo by another actinide cation. At-first contradictory electronic structural data are explained by combining theory and experiment. Complete one-electron transfer from Cp_3U forms the U^{IV}-uranyl(V) compound that behaves as a U^{V}-localized single molecule magnet below 4 K. The extent of reduction by the Cp_3Np group upon oxo-coordination is much less, with a Np^{III}-uranyl(VI) dative bond assigned. Solution NMR and NIR spectroscopy suggest $Np^{IV}U^{V}$ but single-crystal X-ray diffraction and SQUID magnetometry suggest a Np^{III}-U^{VI} assignment. DFT-calculated Hirshfeld charge and spin density analyses suggest half an electron has transferred, and these explain the strongly shifted NMR spectra by spin density contributions at the hydrogen nuclei. The Pu^{III}–U^{VI} interaction is too weak to be observed in THF solvent, in agreement with calculated predictions.*

The uranyl(VI) dication UO_2^{2+} is the most common form of uranium in the environment, and is reduced by minerals and microbes to the less-stable uranyl(V) monocation UO_2^{+}.[1] One of the notable features of the $5f^1$ uranyl(V) ion is its tendency to coordinate to other metal cations through the oxo group, behavior more reminiscent of the heavier f^1 and f^2 neptunyl and plutonyl cations, which form a variety of oxo-bridged cation–cation interactions (CCIs) that interfere with nuclear waste manipulations.[2] Reduction of U^{VI} uranyl to the more Lewis basic U^{V} uranyl ion dramatically increases CCI interactions, providing good models for the behavior of the Np and Pu ions, which are significantly more radioactive than the uranyl ion. Along with the actinyl ions, civil nuclear waste also contains a large number of 5f metal cations from fuel additives and cladding bombardment.[3] Thus, understanding the interaction of uranyl, which represents about 98% of spent fuel, with other 5f metal ions is important.

Simple U^{III} complexes can reduce and activate inert small molecules,[4] but no such reactivity has been reported for transuranic An^{III} complexes in which the An^{IV} formal oxidation state is less thermodynamically favored compared to U^{IV}. However, the reduction of U^{VI} to U^{V} in the uranyl ion is thermodynamically accessible,[5] and recent work by us and others has shown that reduction can be accompanied by oxo-group functionalization with either main group[6] or magnetically more interesting 3d- and 4f- metal cations.[7] The strong anisotropy of the f-block ions has enabled recent breakthroughs in the design of molecular magnets with slow relaxation times that could have applications in spintronic devices, for example.[8] Actinides have been favored over lanthanides in this area due to the relatively greater proportion of covalency (and therefore potential for magnetic communication) in their bonding interactions. Furthermore, the axial symmetry of the uranyl ion offers a design element to control the orientation of the magnetic vector of the single 5f electron in U^{V} uranyl complexes and has been used to construct mixed, oxo-bridged uranyl–transition-metal single molecule magnets (SMMs).[7d]

The difference in preferred coordination geometries of actinyl and actinide cations has been used successfully to make coordination network materials that combine uranium as U^{VI} uranyl and the transuranic neptunium(IV) cation in a phosphate structure,[9] but to the best of our knowledge no reaction to form a heterobimetallic actinide complex through an inner-sphere redox reaction has been reported. We envisaged that the binding and redox-reaction of the uranyl oxo group with potentially reducing f-block metal cations could provide fundamental information on the behavior of actinyl cations in solution, and a versatile and powerful design principle for the synthesis of electronically coupled, redox-active, 5f elements.[7c] Herein we report synthetic routes to the first actinide-functionalized uranyl(V) complexes and a study of their 5f-5f magnetic coupling.

The reaction between THF solutions of [(UO_2)(THF)-(H_2L)] (**A**) and Cp_3An (An = U, Np, Pu, Cp = C_5H_5) results in

[*] Prof. P. L. Arnold, M. S. Dutkiewicz, Dr. M. Zegke, Dr. E. Hollis, Dr. A.-F. Pécharman, Prof. J. B. Love
EaStCHEM School of Chemistry, University of Edinburgh
The King's Buildings, Edinburgh, EH9 3FJ (UK)
E-mail: Polly.Arnold@ed.ac.uk
Jason.Love@ed.ac.uk
M. S. Dutkiewicz, Dr. O. Walter, Dr. C. Apostolidis, Dr. N. Magnani, Dr. J.-C. Griveau, Dr. E. Colineau, Prof. R. Caciuffo
European Commission, Directorate for Nuclear Safety and Security
Joint Research Centre
Postfach 2340, 76125 Karlsruhe (Germany)
E-mail: Roberto.Caciuffo@ec.europa.eu
X. Zhang, Prof. G. Schreckenbach
Department of Chemistry, University of Manitoba
Winnipeg, Manitoba, R3T 2N2 (Canada)
E-mail: Georg.Schreckenbach@umanitoba.ca
Supporting information and the ORCID identification number(s) for the author(s) of this article can be found under: http://dx.doi.org/10.1002/anie.201607022.

a color change of the greenish solution of **A** to brown or red-brown for U and Np, but no observable reaction for the Pu analogue; presumably the Pu cation is insufficiently Lewis acidic and the THF donor solvent thus becomes competitive with Pu-oxo coordination (Scheme 1). For U and Np, crystals of $[Cp_3AnOUO(THF)(H_2L)]$ (An = U, **1a** dark orange; **1b** golden-brown; An = Np, **2a** dark red, **2b** dark red-brown),

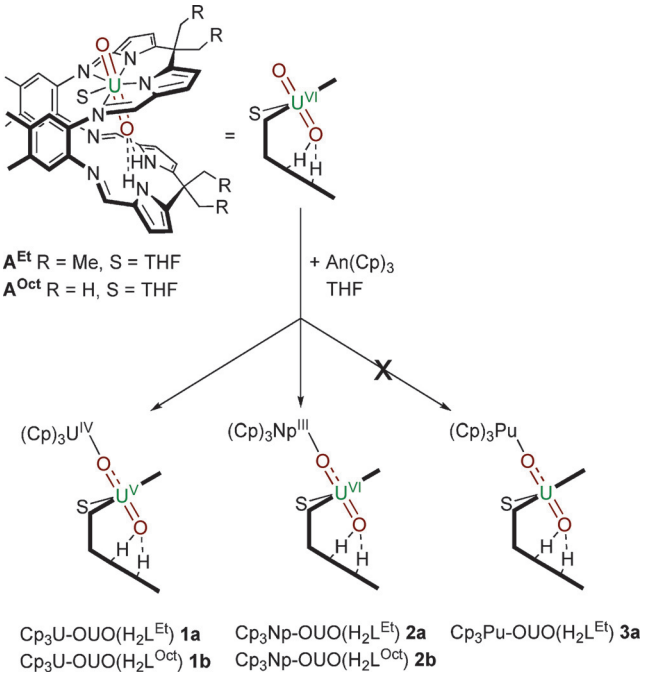

Scheme 1. Reductive oxo-metalation of uranyl complexes by $AnCp_3$ (An = U, Np, Pu).

are isolated in yields of around 30%. All of the complexes are highly air-sensitive, but in general, the octamethyl ligand derivatives (b) are much easier to isolate as they crystallize as large blocks that are readily separable from powdery material. Complexes **2** are the first molecular heterobimetallic uranium-neptunium complexes.

The new An-OUO complexes are exclusively *exo*-oxo metalated, as characterized by ^{1}H NMR, NIR, and IR spectroscopy, and single-crystal X-ray diffraction, and are readily oxidized by trace impurities to form the known An^{IV} complexes $[Cp_3An]_2(\mu\text{-}O)_2$[10] and the U^{VI} uranyl starting material **A**. The solution stability of **2b** is greater than that of **2a**, enabling a full NMR spectroscopic assignment (see the Supporting Information).

In the ^{1}H NMR spectrum of **1a**, the two ligand pyrrole NH protons in the *endo*-cavity resonate at 51.4 ppm (51.1 ppm in **1b**, 55.5 ppm in **2a,** 54.8 ppm in **2b**). These highly paramagnetically shifted resonances, along with other macrocyclic ligand resonances strongly suggest that both Cp_3An^{III} fragments have reduced the uranyl to U^V uranyl forming An^{IV}-U^V uranyl complexes with strong NH–O_{endo} hydrogen-bonding interactions.[5a,11] The resonances for the Cp-ring protons are not similarly diagnostic, however, appearing at 3.17 ppm in **1a** and 3.30 ppm in **1b**. For the pseudo-tetrahedral $[Cp_3U]$-containing complexes reported, the corresponding value for the Cp H is −15.41 ppm in $Cp_3U^{III}(THF)$, with U^{IV} values ranging from −3.48 ppm in $Cp_3U^{IV}Cl$ to −8.8 ppm for $Cp_3U^{IV}(OPh)$ and −18.4 for $Cp_3U^{IV}(OEt)$.[12]

The chemical shift of the Cp protons of −12.1 ppm in **2a** and −11.8 in **2b** are very similar to the Cp ring resonances in the THF-solvated $Cp_3Np^{III}(THF)$ ($\delta_H = -9.65$ ppm) and around 10 ppm higher in frequency than the value of −21.49 ppm in the Np^{IV} complex Cp_3NpCl.[13] Although there is only scant data for comparison, it suggests the Np center is closer in character to Np^{III}, with the uranyl oxo behaving as a donor atom to Np.

The absorption for the uranyl asymmetric stretch is best assigned to uranyl(V) in all four Cp_3U and Cp_3Np complexes in the FTIR spectra with absorptions at 893 cm^{-1} (**1a**), 897 cm^{-1} (**1b**), 892 cm^{-1} (**2a**), and 891 cm^{-1} (**2b**). In each case the value is shifted from that in the parent U^{VI} complex (907 cm^{-1}) in accordance with a weakening of the UO_2 multiple bonding in uranyl(V). Additionally, UV/Vis–NIR spectroscopic characterization of **2** shows several bands characteristic of the C_{3v}-symmetric Cp_3Np^{IV} group (in particular around 1066 and 987 nm)[14] and no evidence of the strong absorption at 1260 nm of $Cp_3Np(THF)$.

Comparison of the solid state structures of **1a** and **2a** (Figure 1), and of **1b** and **2b** (Supporting Information) confirm their isostructurality and all of the metrics argue for formal U^{IV} and U^V uranyl assignment as a result of complete single electron transfer, but are less conclusive for the choice of Np^{III} or Np^{IV} in **2**.

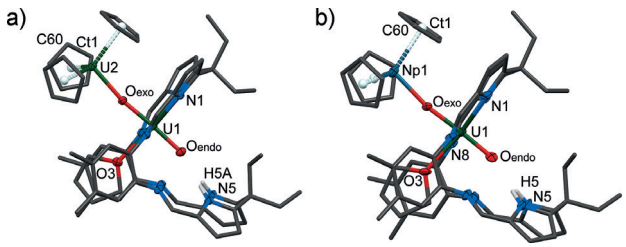

Figure 1. Solid-state structures of a) **1a** and b) **2a**.[23] For clarity, all hydrogen atoms except the pyrrole NHs and all solvent molecules are omitted (ellipsoids are set at 50% probability for non-C/H atoms). Selected bond distances [Å] and angles [°] for **1a**: U1–O_{endo} 1.844(3), U1–O_{exo} 1.986(3), U2–O_{exo} 2.245(3), U2–cent1 2.456, U1–O3 2.503(3), U1–N1 2.464(3), U1–N2 2.673(3), O_{endo}–N5 3.070, U2–C60 2.776(5); O_{exo}-U2-O_{endo} 176.93(12), U1-O_{exo}-U2 171.27(14); for **2a**: U1–O_{endo} 1.826(7), U1–O_{exo} 1.975(7), Np1–O_{exo} 2.249(7), Np1–cent1 2.413, U1–O3 2.496(7), U1–N1 2.450(10), U1–N2 2.459(10), O_{endo}–N5 3.147, Np1–C60 2.724 (9); O_{exo}-U1-O_{endo} 176.9(3), U1-O_{exo}-Np1 170.5(4).

In each case, the uranyl remains linear (O_{exo}-U1-O_{endo} = 178.05(12)° in **1a**, 176.9(3)° in **2a**), and the bimetallic bridge is also almost linear (An-O_{exo}-U1 = 170.70(15)° in **1a**, 170.5(4)° in **2a**). The uranyl ions are equatorially bound by the four macrocyclic N donors, with a coordinated THF molecule in the fifth site. The elongated U=O_{yl} bond lengths in all four structures imply singly reduced U^V uranyl, with a significant lengthening in particular of the metalated *exo*-oxo (in **1a** U–

O_{exo} is 1.976(3) but U–O_{endo} is only 1.840(3) Å). The geometry around the An cation which is coordinated to the *exo*-oxo is unremarkable with approximate C_{3v} symmetry rather than tetrahedral An geometry due to centroid-An-O angles that are smaller than the tetrahedral angle. The average An–C(Cp) distance is 2.733 Å in **1a** and 2.709 Å in **2a**. These data are consistent with a formal oxidation state of U^{IV} as the average U–C distance in $Cp_3U^{IV}(OPh)$ is 2.74 Å,[15] and in $Cp_3U^{III}(THF)$ is 2.79 Å.[12] The average Np–C distance in $Cp_3Np^{IV}(OPh)$ (2.73(3) Å) is somewhat greater than found in **2a** but there are no structurally characterized Np^{III} cyclopentadienyl complexes for comparison. The Cp_3An–O distance in **1a** is 2.245(3) Å and in **2a** is 2.497(7) Å. In **1a** this is consistent with a covalent single bond to U^{IV} although there is a wide range, for example 2.119(7) Å in $Cp_3U^{IV}(OPh)$,[15] and 2.551(10) Å in $Cp_3U^{III}(THF)$.[12] However, in **2a**, this is more consistent with a long single bond or dative bond; the covalent single Np–O bond is 2.136(7) Å in $Cp_3Np^{IV}(OPh)$,[16] whereas the dative Np–O bond in $CpNp^{IV}Cl_3(OP(Me)Ph_2)_2$ is in the range 2.265(12)–2.283(12) Å.[17]

In the anticipation that this synthetic approach could generate actinyl–actinide complexes with magnetic coupling through the bridging oxo group, we have studied the variable-temperature magnetic behavior of **1b** and **2b** by SQUID magnetometry. The dc susceptibility (χ) curves (temperature dependence of χT shown in Figure 2) show that both

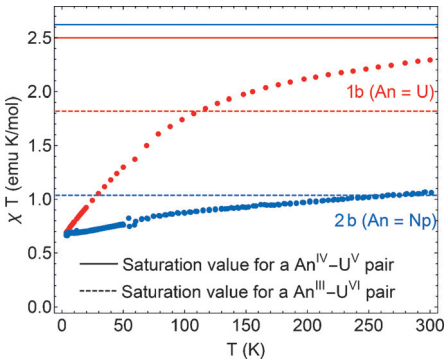

Figure 2. dc magnetic susceptibility (χ) curves measured as a function of temperature (T) for complexes **1b** (red dots) and **2b** (blue dots), plotted as $\chi_{dc}T$ vs. T. Data were collected with an applied field of 1 Tesla. The saturation values expected at high temperature for An^{IV}–U^{V} and An^{III}–U^{VI} pairs are also plotted (in blue for An = Np and in red for An = U) as continuous and dashed lines, respectively.

complexes have an effective magnetic moment around 2.4 μ_B at low temperature, but upon increasing the temperature, their behavior differs. While the χT product for **1b** rapidly increases well above the upper theoretical limit expected for a U^{III}–U^{VI} pair, and at room temperature approaches the expected value for a U^{IV}–U^{V} pair, the effective moment for **2b** slowly reaches the value corresponding to a Np^{III}–U^{VI} pair and tends to saturate without increasing further. This indicates that the electron transfer in the Np–U **2b** adduct is extremely poor, whereas reduction of the uranyl group has taken place in the U–U analogue **1b**.

Because of this, we have investigated the dynamic magnetic properties of **1b** by ac magnetic susceptibility measurements (Figure 3). Clear peaks in the out-of-phase component of the ac susceptibility indicate that slow magnetic relaxation takes place and that **1b** behaves as a single-

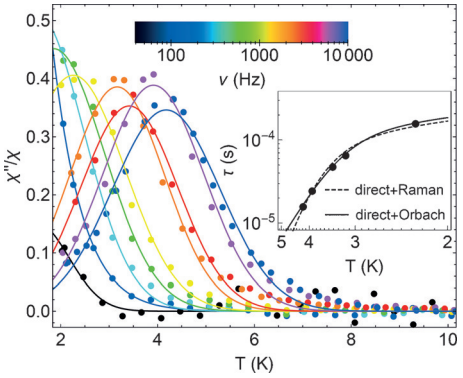

Figure 3. Out-of-phase component of the ac magnetic susceptibility (χ'') for **1b** measured as a function of temperature, for various values of the frequency ν of the 5 G driving field. The plot shows χ''/χ_{dc} vs. T curves, since the relaxation time τ becomes equal to $(2\pi\nu)^{-1}$ exactly at the temperature, which corresponds to the peak in χ''/χ.[19] The values of τ derived with this procedure are shown in the inset as a function of temperature in a log–reciprocal plot, together with curve fits obtained considering, respectively a Raman (•••••) and an Orbach (——) relaxation path in addition to a direct process (see the Supporting Information for details).

molecule magnet below 4 K. The temperature dependence of the relaxation time τ can be fitted equally well to a Raman or an Orbach relaxation pathway, in addition to a direct process; however, we note that both the characteristic time $\tau_0 = 3.26 \times 10^{-8}$ s and the thermal activation barrier $\Delta = 26.9$ K are very similar to previously reported U^{V} based single-ion magnets.[18] This, together with the consideration that U^{IV} is often non-magnetic in low-symmetry geometries, and with the absence of any clear sign of magnetic interaction between the two uranium sites in the susceptibility curves, allows us to attribute the slow magnetic relaxation to the uranyl(V) group. We note that a more symmetrical heterodimetallic uranyl(V)–Mn^{II} complex has the highest reported relaxation barrier for a mono-U^{V} system, of 81 ± 0.5 K, which is presumably due to the high Ising anisotropy.[7a]

It is therefore clear that not all of the experimental characterization data agree on the extent of electron transfer from the organometallic actinide to the uranyl group:

- NMR: The paramagnetic shifting of the resonances in the macrocyclic ligand in both **1** and **2** is suggestive of singly reduced uranyl(V) in both. The paramagnetic chemical shifts of the Cp ring protons are less diagnostic; in the U–U complexes **1** the chemical shift of the Cp protons is similar to most U^{IV} complexes, whereas those in the Np–U complexes **2** are comparable with those of some Np^{III} cyclopentadienyl complexes.
- NIR–UV/Vis–IR: The vibrational data support U^{IV}–U^{V} oxidation states for **1** and Np^{IV}–U^{V} oxidation states for **2**.

- XRD: The crystal structures of both the Cp_3An–(OUO) systems are isostructural, and present convincing evidence for single electron transfer in **1** but less so in **2**. The data show characteristic elongation of the U–(μ-O)–An distances and to smaller extent also U–O(*endo*), suggestive of the uranyl(V) ion in both but the An–O_{exo} uranyl distances are more in line with U^{IV} and Np^{III} formal oxidation state assignments.
- SQUID magnetometry: For **1b** the data are consistent with full electron transfer to form a U^{IV}–U^{V} complex. However, for **2b** the magnetic ground state saturation values closely match those of the isolated Np^{III} ion, suggesting a donor–acceptor oxo bridged Np^{III}–U^{VI} product.

DFT calculations on models of **1b** to **3b** help with the bond type assignments and support the proposed decreasing level of electron transfer from Cp_3U through Cp_3Pu. The Gibbs free energies for each reaction in Scheme 1 were calculated (Supporting Information, Table S3) and the positive gas-phase value (2.81 kcal mol^{-1}) for Cp_3Pu suggests the reaction to form **3b** is unfavorable. The calculated uncorrected, gas-phase Cp_3An^{IV}/Cp_3An^{III} reduction potentials vs. ferrocene (Supporting Information, Table S4) are −1.21 eV for U, −0.81 eV for Np, and −0.41 eV for Pu and follow the same trend as the experimental data, that is, the reduction of Cp_3AnCl is −1.80 V for U^{IV} and −1.29 V for Np^{IV} in THF vs. ferrocene.[20] We previously measured the relatively facile reduction of the uranyl complex $\mathbf{A^{Oct}}$ as −1.18 V vs. ferrocene in THF solution[21] and so comparison of these reduction potentials predicts that it will be more difficult to transfer an electron from Cp_3Np^{III} than Cp_3U^{III}. The calculated charges and spin densities on the An and uranium centers (Supporting Information, Tables S5 and S6) agree with the oxidation states assigned by SQUID magnetometry, with the spin density on the U^{V} centers decreasing in the order **1** > **2** > **3** because all the unpaired electrons in these systems are very localized (Supporting Information, Figures S12–S14). Thus, the extent of electron transfer can be deduced by comparing the separated fragments Cp_3An^{III} and $U^{VI}O_2(H_2L^{Oct})$ to the final products **1b**/**2b**/**3b** (Supporting Information, Table S6). The spin density analyses indicate that the U–U system (**1**) has complete one-electron transfer but in contrast Np–U(**2**) and Pu–U(**3**) have just half. An orbital composition analysis (Supporting Information, Table S7) shows that the three SOMOs in the U–U complex **1b** have f with minor d contributions. The Np–U system (**2b**) is similar, but has non-negligible s character in a singly occupied orbital which may contribute to the observed paramagnetically shifted ^{1}H NMR spectrum. More importantly in this respect, the spin density on the Cp hydrogen atoms (Supporting Information, Table S8) is on average twice that of the U system.[22]

To conclude, we report herein the first reduction of the uranyl dication by another actinide complex, and the first use of a redox reaction to generate a heterobimetallic transuranic complex. For the more reducing An^{III} ions the oxo group provides a capable bridge between the two actinide cations. Although there is some disagreement between techniques as to the formal oxidation states, in combination they show that the extent of electron transfer to the uranyl is U > Np > Pu. There is no apparent magnetic communication between the actinide centers in these $Cp_3An(UO_2)$ systems, and the U^{IV}–U^{V} complex **1b** is a single-ion magnet (singly reduced uranyl, d^0f^1), with a relaxation barrier of 19 cm^{-1} and relaxation time of 2.5×10^{-8} s at infinite temperature. A strong donor–acceptor interaction, or perhaps even non-integral formal oxidation states for Np and U, are probably most appropriate for **2**. Somewhat surprisingly, any interaction between the Pu^{III} and U^{VI} is too weak to be observed in the presence of coordinating THF solvent, and calculated free energies suggest that the reaction is unlikely to happen. Characterizing paramagnetic actinide complexes with complicated electronic structures is very challenging even with modern techniques, and at first glance the classical interpretations of the data give contradictory pictures. However, we have shown how a satisfying electronic structure can be defined by a combined experimental and computational analysis. This new synthetic route should provide opportunities for new uranyl functionalization with other f-block metal cations to form other unusual and potentially interesting f-electron behaviors.

Acknowledgements

The experiments were supported by the EPSRC-UK (EP/M010554/1, EP/H0048231), the University of Edinburgh, the EU Actinet-I3-AC3-JRP-02 and Talisman Joint Research Project under contract with the European Commission. P.L.A. also thanks the Technische Universität München—Institute for Advanced Study, funded by the German Excellence Initiative. M.S.D. acknowledges the European Commission for support in the frame of the Training and Mobility of Researchers programme. G.S. acknowledges funding from NSERC (Discovery Grant). We also thank Marketa Suvova and Dr. Nicola Bell for some of the spectroscopic characterization of $\mathbf{A^{Et}}$ and **1a**.

Keywords: macrocycles · neptunium · plutonium · redox reactions · uranyl cations

How to cite: *Angew. Chem. Int. Ed.* **2016**, *55*, 12797–12801
Angew. Chem. **2016**, *128*, 12989–12993

[1] P. L. Arnold, J. B. Love, D. Patel, *Coord. Chem. Rev.* **2009**, *253*, 1973.
[2] B. Vlaisavljevich, P. Miró, D. Ma, G. E. Sigmon, P. C. Burns, C. J. Cramer, L. Gagliardi, *Chem. Eur. J.* **2013**, *19*, 2937.
[3] a) L. Natrajan, F. Burdet, J. Pécaut, M. Mazzanti, *J. Am. Chem. Soc.* **2006**, *128*, 7152; b) G. Nocton, P. Horeglad, J. Pécaut, M. Mazzanti, *J. Am. Chem. Soc.* **2008**, *130*, 16633.
[4] P. L. Arnold, *Chem. Commun.* **2011**, *47*, 9005.
[5] a) P. L. Arnold, A.-F. Pécharman, R. M. Lord, G. M. Jones, E. Hollis, G. S. Nichol, L. Maron, J. Fang, T. Davin, J. B. Love, *Inorg. Chem.* **2015**, *54*, 3702; b) P. L. Arnold, A.-F. Pecharman, E. Hollis, A. Yahia, L. Maron, S. Parsons, J. B. Love, *Nat. Chem.* **2010**, *2*, 1056.
[6] a) E. A. Pedrick, G. Wu, T. W. Hayton, *Inorg. Chem.* **2014**, *53*, 12237; b) G. M. Jones, P. L. Arnold, J. B. Love, *Chem. Eur. J.* **2013**, *19*, 10287; c) D. D. Schnaars, G. Wu, T. W. Hayton, *Inorg. Chem.* **2011**, *50*, 4695.

[7] a) L. Chatelain, J. P. S. Walsh, J. Pécaut, F. Tuna, M. Mazzanti, *Angew. Chem. Int. Ed.* **2014**, *53*, 13434; *Angew. Chem.* **2014**, *126*, 13652; b) P. L. Arnold, E. Hollis, G. S. Nichol, J. B. Love, J.-C. Griveau, R. Caciuffo, N. Magnani, L. Maron, L. Castro, A. Yahia, S. O. Odoh, G. Schreckenbach, *J. Am. Chem. Soc.* **2013**, *135*, 3841; c) P. L. Arnold, E. Hollis, F. J. White, N. Magnani, R. Caciuffo, J. B. Love, *Angew. Chem. Int. Ed.* **2011**, *50*, 887; *Angew. Chem.* **2011**, *123*, 917; d) V. Mougel, L. Chatelain, J. Pécaut, R. Caciuffo, E. Colineau, J.-C. Griveau, M. Mazzanti, *Nat. Chem.* **2012**, *4*, 1011.

[8] J. D. Rinehart, J. R. Long, *Chem. Sci.* **2011**, *2*, 2078.

[9] A.-G. D. Nelson, T. H. Bray, T. E. Albrecht-Schmitt, *Angew. Chem. Int. Ed.* **2008**, *47*, 6252; *Angew. Chem.* **2008**, *120*, 6348.

[10] M.-R. Spirlet, J. Rebizant, C. Apostolidis, E. Dornberger, B. Kanellakopulos, B. Powietzka, *Polyhedron* **1996**, *15*, 1503.

[11] M. Zegke, G. S. Nichol, P. L. Arnold, J. B. Love, *Chem. Commun.* **2015**, *51*, 5876.

[12] H. J. Wasserman, A. J. Zozulin, D. C. Moody, R. R. Ryan, K. V. Salazar, *J. Organomet. Chem.* **1983**, *254*, 305.

[13] Re-recorded by us in [D_6]benzene on a modern spectrometer. ^{1}H NMR (C_6D_6, 293.1 K, 400.33 MHz): −21.49 (s, 15 H) ppm.

[14] R. Bohlander, Universität Karlsruhe (Germany. Institut für Heiße Chemie; Kernforschungszentrum, Fakultät für Chemie), **1986**.

[15] M. R. Spirlet, J. Rebizant, C. Apostolidis, G. Van den Bossche, B. Kanellakopulos, *Acta Crystallogr. Sect. C* **1990**, *46*, 2318.

[16] D. J. A. De Ridder, C. Apostolidis, J. Rebizant, B. Kanellakopulos, R. Maier, *Acta Crystallogr. Sect. C* **1996**, *52*, 1436.

[17] K. W. Bagnall, G. F. Payne, N. W. Alcock, D. J. Flanders, D. Brown, *J. Chem. Soc. Dalton Trans.* **1986**, 783.

[18] D. M. King, F. Tuna, J. McMaster, W. Lewis, A. J. Blake, E. J. L. McInnes, S. T. Liddle, *Angew. Chem. Int. Ed.* **2013**, *52*, 4921; *Angew. Chem.* **2013**, *125*, 5021.

[19] N. Ishikawa, M. Sugita, T. Ishikawa, S.-y. Koshihara, Y. Kaizu, *J. Phys. Chem. B* **2004**, *108*, 11265.

[20] D. C. Sonnenberger, J. G. Gaudiello, *Inorg. Chem.* **1988**, *27*, 2747.

[21] J. J. Berard, H. G. Schreckenbach, P. L. Arnold, D. Patel, J. B. Love, *Inorg. Chem.* **2008**, *47*, 11583.

[22] J. Autschbach in *Annual Reports in Computational Chemistry*, *Vol. 11* (Ed.: A. D. David), Elsevier, Dordrecht, **2015**, p. 3.

[23] CCDC 1490124 – 1490128 contain the supplementary crystallographic data for this paper. These data are provided free of charge by The Cambridge Crystallographic Data Centre.

Received: July 20, 2016
Published online: September 15, 2016

